Phytomedicine 145 (2025) 157057

Contents lists available at ScienceDirect

Phytomedicine

journal homepage: www.elsevier.com/locate/phymed

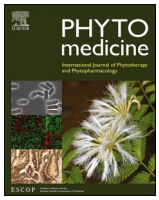

Original Article

Lycopene ameliorates Di-(2-ethylhexyl) phthalate-induced neurotoxicity in mice via the gut-brain axis

Li-Jian Chen [a,1], Yi Liu [b,1], Jia-Li Liu [b,1], Zhi-Jiang Chen [a], Wei Zhao [a], Ji-Hui Li [b], Clare Hsu [b], Long Chen [b], Jia-Hao Zeng [b], Xiu-Wen Li [c], Jian-Zheng Yang [b], Jia-Hao Li [b], Xiao-Li Xie [c], Shao-Hua Tao [a,*], Qi Wang [a,*]

[a] Department of Pediatric Intensive Medicine, Zhujiang Hospital, Southern Medical University, Guangzhou, Guangdong, 510280, China
[b] Guangzhou Key Laboratory of Forensic Multi-Omics for Precision Identification, School of Forensic Medicine, Southern Medical University, Guangzhou, Guangdong, 510515, China
[c] Department of Toxicology, School of Public Health, Southern Medical University (Guangdong Provincial Key Laboratory of Tropical Disease Research), Guangzhou, Guangdong 510515, China

ARTICLE INFO

Keywords:
Di(2-ethylhexyl) phthalate
Lycopene
Neurotoxicity
Gut microbiota
NOD-like receptor signaling pathway
Gut-brain axis

ABSTRACT

Background: Di(2-ethylhexyl) phthalate (DEHP), a ubiquitous plasticizer present in numerous consumer products, poses a substantial neurotoxic risk through environmental and dietary exposure. Growing evidence highlights a critical association between DEHP-induced neurotoxicity and gut microbiota dysbiosis. Renowned for its potent antioxidant and anti-inflammatory capabilities, the natural carotenoid lycopene (Lyc) demonstrates therapeutic promise in treating various neurological disorders.

Purpose: The potential neuroprotective mechanisms of Lyc against DEHP-induced neurotoxicity in mice were investigated in this study, with a specific focus on its interaction with the gut-brain axis.

Methods: For 35 consecutive days, mice received daily intragastric administrations of DEHP or Lyc. A comprehensive approach involving integrated transcriptome, microbiome, and molecular biology analyses, in conjunction with bacteriotherapy, was utilized to thoroughly investigate the underlying mechanisms.

Results: Our findings demonstrated that Lyc administration or fecal microbiota transplantation (FMT) from Lyc-treated mice effectively ameliorated DEHP-induced anxiety- and depression-like behaviors. At the molecular level, Lyc mitigated neuroinflammation in the hippocampus, potentially through modulation of the NOD-like receptor signaling pathway. Furthermore, Lyc treatment improved gut microbiota composition by promoting the growth of beneficial bacteria, such as *Akkermansiaceae*, and enhanced intestinal barrier integrity via increased expression of tight junction proteins. Lyc also regulated the LPS-TLR4/MyD88 signaling pathway in the colon, thereby reducing local inflammation.

Conclusion: These results provide compelling evidence that Lyc confers protection against DEHP-induced neurotoxicity through a multifaceted strategy involving modulation of gut-brain axis, suppression of neuroinflammation, and restoration of gut homeostasis. We propose a novel therapeutic strategy to alleviate the risks posed by DEHP to both neurological and intestinal health. This approach involves either supplementation with Lyc or the application of bacteriotherapy.

Introduction

Di-(2-ethylhexyl) phthalate (DEHP), a commonly utilized plasticizer, is a pervasive environmental contaminant found in an extensive range of consumer products, from packaging for food and medical equipment to kids' toys (Erythropel et al., 2014). Its widespread application and lipophilic nature facilitate its leaching into food, water, and air, leading to human exposure primarily through ingestion, inhalation, and skin absorption (Zhang et al., 2022). Chronic DEHP exposure has been linked to diverse adverse health outcomes across various organ systems, such as the brain, liver, kidneys, spleen, and reproductive tract (Kang et al., 2021; Wang et al., 2023; Wu et al., 2022; Yang et al., 2021). Mounting

* Corresponding authors at: Department of Pediatric Intensive Medicine, Zhujiang Hospital, Southern Medical University, Guangzhou, Guangdong, 510280, China.
E-mail addresses: tsh1987@sina.com (S.-H. Tao), wangqi1980@smu.edu.cn (Q. Wang).
[1] These authors contributed equally to this work.

https://doi.org/10.1016/j.phymed.2025.157057
Received 27 November 2024; Received in revised form 23 June 2025; Accepted 4 July 2025
Available online 5 July 2025

evidence particularly highlights DEHP's neurotoxic potential. Studies in murine models report behavioral abnormalities, including anxiety- and depression-like behaviors, following exposure (Wang et al., 2016). Another research reported that DEHP exposure led to changes in brain morphology, cognitive impairments, motor function deficits, and compromised blood-brain barrier function (Zhao et al., 2024). These neurotoxicity effects are thought to be mediated by various mechanisms, although the precise molecular pathways remain to be fully elucidated.

The gut-brain axis is fundamental for ensuring homeostasis and regulating different physiological processes, including behavior and mental state (CRYAN and DINAN, 2012). This complex network involves interactions among the gut microbiota, the intestinal epithelium, the immune system, and the CNS, mediated by neural, endocrine, and immune signaling pathways. Furthermore, recent research has underscored the impact of DEHP exposure on gut microbiota (Su et al., 2022), indicating that modifications within the gut-brain axis could contribute to DEHP associated neurotoxicity. DEHP has been shown to induce learning and memory deficits via the gut-brain axis by down-regulating TPH1 in intestinal epithelial cells and diminishing gut microbiota diversity and abundance, subsequently decreasing 5-HT secretion (Wang et al., 2023). Exposure to DEHP can significantly change the structure and function of the gut microbiota community (Lei et al., 2019), potentially resulting in the creation of toxic metabolites that contribute to neurodevelopmental disorders. For instance, DEHP exposure has been shown to induce oxidative stress injury in the jejunum, resulting in compromised tissue integrity, tight junction damage, and alterations in the intestinal flora (Zhao et al., 2020). Moreover, gut microbiota dysbiosis has been implicated in DEHP-induced cholesterol imbalance (Yu et al., 2021). This complex interplay among DEHP exposure, gut microbiota dysbiosis, and neurobehavioral changes warrants further investigation.

Lycopene (Lyc), a naturally present carotenoid pigment abundant in tomatoes and various red-colored fruits and vegetables, has garnered substantial interest due to the diverse biological activities and potential health benefits (Long et al., 2024). Due to its potent antioxidant and anti-inflammatory properties, Lyc has been shown to exert protective effects against various diseases, including cancer, cardiovascular disease, and metabolic disorders (Imran et al., 2020; Ozkan et al., 2023). Furthermore, accumulating evidence suggests a promising role for Lyc in mitigating neurotoxicity and neurodegenerative processes. Lyc's neuroprotective mechanisms are believed to involve reducing oxidative stress, modulating inflammatory responses, regulating the hypothalamic-pituitary-adrenal axis, and modulating monoamine neurotransmitter levels (Wu et al., 2022). Lyc can also prevent hepatotoxicity induced by DEHP through mitigating damage from oxidative stress and CYP450 dysfunctions via the AHR and Nrf2 pathways (Zhao et al., 2021). Furthermore, Lyc has exhibited protective effects against DEHP-induced toxicity in other organs, including the brain, where it has been proven to alleviate DEHP-related cognitive impairment via modulating iron accumulation and glutathione metabolism (Wang et al., 2023). These findings collectively indicates that Lyc may offer a promising strategy for counteracting the detrimental effects of DEHP exposure, particularly in the context of neurotoxicity.

Lyc has been demonstrated to modulate both the NF-κB-NLRP3 pathway and gut microbiota in mice on high-fat and high-fructose diets, thereby preventing the development of nonalcoholic fatty liver disease (Gao et al., 2023). Lyc can also relieve DSS-induced colitis and associated behavioral disorders via rebalancing the microbe-gut-brain axis (Zhao et al., 2020). These findings indicated a possible function for the gut-brain axis in mediating the neurotoxic effects of DEHP and suggest that Lyc may provide neuroprotective effects by modulating the gut microbiota. However, the specific mechanisms by which lycopene modulates the gut-brain axis in the context of DEHP-induced neurotoxicity remain poorly understood.

The aim of the current research was to explore the potential neuroprotective effects of Lyc against DEHP-induced neurotoxicity in mice, emphasizing the importance of the gut-brain connection. We hypothesized that Lyc would mitigate DEHP-induced neurobehavioral deficits, neuroinflammation, and systemic inflammation and oxidative stress by regulating gut microbiota composition, enhancing intestinal barrier integrity, and regulating key signaling pathways involved in inflammation and gut homeostasis. To test this hypothesis, we employed a comprehensive approach integrating behavioral testing, biochemical assays, mRNA sequencing of hippocampal tissue, 16S ribosomal RNA (16S rRNA) gene sequencing of the gut microbiota, bacteriotherapy, and other relevant biological detection techniques. This multifaceted approach enabled us to explore the complex interplay among DEHP exposure, gut microbiota dysbiosis, and neurobehavioral changes, and to elucidate the potential mechanisms underlying Lyc's protective effects via the microbiota-gut-brain axis.

Materials and methods

Chemical reagents

DEHP (purity > 99 %, CAS: 117–81–7), Lyc (purity > 95 %, CAS: 502–65–8), and Fluoxetine (Flu, purity > 98 %, CAS: 56296–78–7) were obtained from Sigma-Aldrich Corporation (St. Louis, MO, USA). The chemical structures of DEHP, Lyc, and Flu are presented in Fig. S1A-C.

Animals

Adult male C57BL/6 mice (6–8 weeks, 22 ± 2 g), were obtained from the Laboratory Animal Center of Southern Medical University. All experimental procedures adhered to institutional animal experimentation ethical guidelines and received approval from the Medical Ethics Committee of Southern Medical University (Approval Code: L2023005, registered on March 13, 2023).

Animal treatment and experimental design

After acclimation in environment for a week, mice were randomly assigned to 8 experimental groups as follows: control group (Control), DEHP group (DEHP), Lyc group (Lyc), DEHP+Lyc 2.5mg/kg group (DEHP+L1, L1 = Lyc 2.5 mg/kg), DEHP+Lyc 5mg/kg group (DEHP+L2, L2 = Lyc 5 mg/kg), DEHP+Lyc 10mg/kg group (DEHP+L3, L3 = Lyc 10 mg/kg), DEHP+Flu 20mg/kg group (DEHP+Flu), and DEHP+fresh fecal samples from the Lyc (5 mg/kg) treated group (DEHP+FMT-L2). Briefly, (1) Control: Administered corn oil via gavage; (2) DEHP: Administered DEHP (200 mg/kg BW/day) via gavage; (3) Lyc: Administered Lyc (5 mg/kg BW/day) via gavage; (4) DEHP+L1: Co-administered DEHP (200 mg/kg BW/day) and Lyc (2.5 mg/kg BW/day) via gavage; (5) DEHP+L2: Co-administered DEHP (200 mg/kg BW/day) and Lyc (5 mg/kg BW/day) via gavage; (6) DEHP+L3: Co-administered DEHP (200 mg/kg BW/day) and Lyc (10 mg/kg BW/day) via gavage; (7) DEHP+Flu: Co-administered DEHP (200 mg/kg BW/day) and Fluoxetine (Flu, 20 mg/kg BW/day) via gavage. DEHP, Lyc, and Flu were dissolved in corn oil and 10 ml/kg body weight of the solution was administered per mouse. (8) DEHP+FMT-L2: Co-administered DEHP (200 mg/kg BW/day) and fresh fecal samples from the Lyc (5 mg/kg) treated group via gavage (FMT-recipient mice). For the FMT-donor, fecal samples were freshly collected from Lyc (5 mg/kg BW/day) mice under SPF conditions and stored in sterile tubes. The feces were diluted in sterile phosphate-buffered saline after being weighed (100 mg/ml), centrifuged at 900 × *g* for 3 min, and 0.2 ml of the supernatant was administered per mouse (Zhang et al., 2023). To ensure the bacterial viability, donor stool was freshly prepared on the day of transplant within two hours before gavage administration (Jing et al., 2021). All substances (vehicle, DEHP, Lyc, Flu, or FMT) were administered intragastrically (via gavage) once daily for 35 consecutive days. The DEHP dose (200 mg/kg) was chosen based on previous studies demonstrating its effectiveness in inducing anxiety- and depression-like behaviors for mechanistic analysis (Kang

et al., 2021). Many studies have shown that 5 mg/kg Lyc alleviates the toxicity associated with DEHP, including neurotoxicity (Wang et al., 2023), nephrotoxicity (Li et al., 2023), splenic toxicity (Dai et al., 2022), hepatotoxicity (Zhao et al., 2021), reproductive toxicity (Zhao et al., 2022), and cardiotoxicity (Cui et al., 2022). In the present study, we used three Lyc concentrations (2.5, 5, and 10 mg/kg) for intervention. Fluoxetine at 20 mg/kg is a well-established dose for its anxiolytic and antidepressant effects (He et al., 2024; Wang et al., 2025).

Behavior tests

Following 35 days of DEHP and/or Lyc administration, behavioral tests were conducted to evaluate anxiety and depression. The open field test (OFT) and the elevated plus maze (EPM) test were used to evaluate anxiety-like behavior. To evaluate depression-like behavior, researchers employed the tail suspension test (TST) and the forced swim test (FST), both standard assays for this purpose. The experimental procedures are detailed in the Supplementary material.

Sample collection

Mouse feces were collected in metabolic cages within 24 h of the final gavage and immediately snap-frozen at −80 °C. Animals were then euthanized under anesthesia with 0.3 % pentobarbital sodium (45 mg/kg i.p.), followed by blood collection by cardiopuncture. After euthanasia, the entire colon was carefully dissected, and its length was measured from the cecum to the rectum/anus using a standard ruler. Hippocampal and colon tissues were gathered and either kept at −80 °C or fixed with 4 % paraformaldehyde for subsequent analysis. Serum was obtained by centrifuging blood samples at 12,000 × *g* for 10 min at 4 °C and then stored at −80 °C for subsequent biochemical analysis.

Enzyme-linked immunosorbent assays (ELISAs)

Levels of TNF-α, IL-1β, IL-6, MDA, ROS, and LPS in serum were measured using commercially available ELISA kits according to the manufacturer's instructions. The catalog number information of ELISA kits are listed in the Supplementary material.

Histopathological analyses

After 48 h of fixation, colon tissues were dehydrated using an automatic tissue processor, embedded in paraffin, and sectioned at 3 μm with a microtome (Leica) for mounting on slides. Specific staining procedures, including hematoxylin-eosin (H&E), alcian blue-periodic acid Schiff (AB-PAS), and IHC, are shown in the Supplementary material.

RNA sequencing and bioinformatics analyses

RNA-seq was performed by Majorbio Bio-Pharm Technology Co. Ltd. (Shanghai, China). The comprehensive methods for experiments and data analysis methods were outlined in the Supplementary material.

16S rRNA gene sequencing and data analysis

16S rRNA gene sequencing was carried out by Majorbio Bio-Pharm Technology Co. Ltd. (Shanghai, China). The Supplementary material describes the detailed methods used for experiments and data analysis.

RT-qPCR analysis

Amplification and quantification were subsequently performed on the Roche LightCycler 96 System (Roche, Switzerland), utilizing SYBR green reagents and specific primers (Supplementary Table 1) in combination with the cDNA templates. Detailed procedures for experiments and data analysis were presented in the Supplementary material.

Western blotting analysis

Primary antibodies included *p*-P65 (Cat# 3033, 1:1000, CST), P65 (Cat# 8242, 1:1000, CST), NLRP3 (Cat# T55651S, 1:1000, Abmart), TLR4 (Cat# sc293072, 1:1000, Santa Cruz Biotechnology), MyD88 (Cat# BD-PT2928, 1:1000, Biodragon), ZO-1 (Cat# AF5145, 1:1,1000, Affinity Biosciences), Occludin (Cat# 13,409–1-AP, 1:1,1000, Proteintech), and β-Actin (Cat# 66,009–1-Ig, 1:10,000, Proteintech). Secondary antibodies were HRP-labeled goat anti-mouse IgG ($H + l$) or anti-rabbit IgG ($H + l$) (Cat# IH-0031 or Cat# IH-0011, 1:10,000, Beijing Dingguo Changsheng Biotechnology). The methods for conducting experiments and analyzing data are thoroughly explained in the Supplementary material.

Statistical analysis

Data analysis was performed using GraphPad Prism software (version 9.0) and is expressed as mean ± standard error of the mean (SEM). For multiple group comparisons, one-way analysis of variance (ANOVA) was utilized, followed by Tukey's post hoc test. Statistical significance was defined as a P value below 0.05 ($^{*}p < 0.05$, $^{**}p < 0.01$, $^{***}p < 0.001$, $^{****}p < 0.0001$; ns, not statistically significant). Both RNA-seq and 16S rRNA gene sequencing datasets were analyzed on the freely accessible Majorbio Cloud platform (https://cloud.majorbio.com).

Results

Lyc alleviates DEHP-induced anxiety-like and depression-like behavior, neuroinflammation and oxidative stress

To evaluate Lyc's therapeutic efficacy against DEHP-induced neurotoxicity, a murine model was established by administering DEHP for 35 days. Lyc was administered orally across a range of doses (2.5, 5, and 10 mg/kg), with Fluoxetine (Flu) at 20 mg/kg serving as a positive control (Fig. 1A). Anxiety- and depression-like behaviors were assessed using the OFT, EPM, TST, and FST, respectively. Five weeks of DEHP exposure significantly reduced total distance traveled, entries into the center zone, and time spent in the center zone during the OFT (Fig. 1B-C), decreased by 39.7 %, 47.4 %, and 50 %, respectively. Concurrently, DEHP increased entries into and time spent in the closed arms of the EPM (Fig. 1D-E), increased by 116 % and 27.2 %, respectively, indicative of anxiety-like behavior. Notably, Lyc (5 and 10 mg/kg) and Flu treatment significantly reversed these effects, increasing total distance traveled (increased by 36.4 %, 47.3 %, and 40.9 %, respectively), center entries (increased by 58.4 %, 71.1 %, and 34.8 %, respectively), and time in the center (increased by 55.7 %, 117 %, and 66.4 %, respectively) in the OFT (Fig. 1B-C), and decreasing entries into (decreased by 33.9 %, 46.8 %, and 47.8 %, respectively) and time spent in the closed arms (decreased by 15.8 %, 19.0 %, and 17.9 %, respectively) of the EPM (Fig. 1D-E). In the TST and FST, DEHP exposure significantly prolonged immobility time, increased by 31.4 % and 48.9 %, respectively (Fig. 1F-G), suggesting the development of depression-like behavior. Lyc (5 and 10 mg/kg) and Flu reduced immobility time in TST (decreased by 12.7 %, 15.7 %, and 27 %, respectively) and FST (decreased by 20.3 %, 18.3 %, and 21.2 %, respectively) (Fig. 1F-G), indicating an alleviation of depression-like behavior. However, Lyc at 2.5 mg/kg failed to improve anxiety- or depression-like behaviors (Fig. 1B-G). Collectively, these findings demonstrate that Lyc (5 and 10 mg/kg) and Flu effectively alleviate DEHP-induced anxiety- and depression-like behaviors. Furthermore, neuronal damage in the hippocampus was assessed using H&E staining. H&E staining revealed a general increase in pyknotic nuclei within the cornu ammonis (CA)1, CA3, and dentate gyrus (DG) regions of the hippocampus in the DEHP group compared to the Control, Lyc, DEHP+L1, DEHP+L2, DEHP+L3, and DEHP+Flu groups (Fig. S2A). These pathological changes were

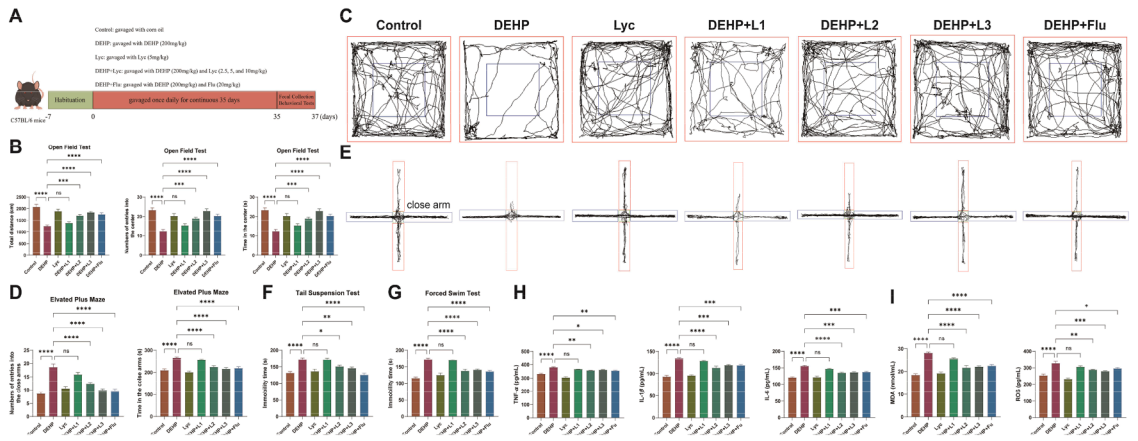

Fig. 1. Effects of Lyc on DEHP-induced abnormal behavior, neuroinflammation and oxidative stress. (A) Experimental period schematic diagram (By Figdraw. https://www.figdraw.com). (B) OFT: total distance, numbers of entries into the center and time in the center. $n = 10$ per group. (C) Trace representation of the OFT; (D) EPM: numbers of entries into the close arms and time in the close arms. $n = 10$ per group. (E) Representative tracks of the EPM; (F, G) Duration of immobility in the TST (F) and FST (G). $n = 6$–8 per group. (H, I) Serum levels of inflammatory cytokines (TNF-α, IL-1β, and IL-6) and oxidative stress markers (MDA and ROS). $n = 4$ per group. The data represent the mean ± SEM and were analyzed using one-way ANOVA (Tukey post hoc test), and statistical significance was determined by $P < 0.05$. *$P < 0.05$, **$P < 0.01$, ***$P < 0.001$, ****$P < 0.0001$ and ns, not statistically significant.

substantially mitigated following Lyc (5 and 10 mg/kg) and Flu treatment. Overall, these results suggest that Lyc (5 and 10 mg/kg) and Flu exert protective effects against DEHP-induced nervous system injury.

Given the established link between neuroinflammation, oxidative stress, and anxiety/depression-like behaviors (Beheshti et al., 2020; Patki et al., 2013), we quantified serum concentrations of inflammatory cytokines (TNF-α, IL-1β, and IL-6) and oxidative stress indicators (MDA and ROS). DEHP exposure significantly elevated TNF-α, IL-1β, IL-6, MDA, and ROS in serum (Fig. 1H-I). Conversely, Lyc (5 and 10 mg/kg) and Flu treatment significantly reduced these DEHP-induced elevations (Fig. 1H-I). Lyc at 2.5 mg/kg was less effective (Fig. 1H-I). Serum inflammatory cytokine levels correlated positively with oxidative stress markers (Fig. S2B), suggesting a link between increased inflammation and elevated oxidative stress. These findings collectively

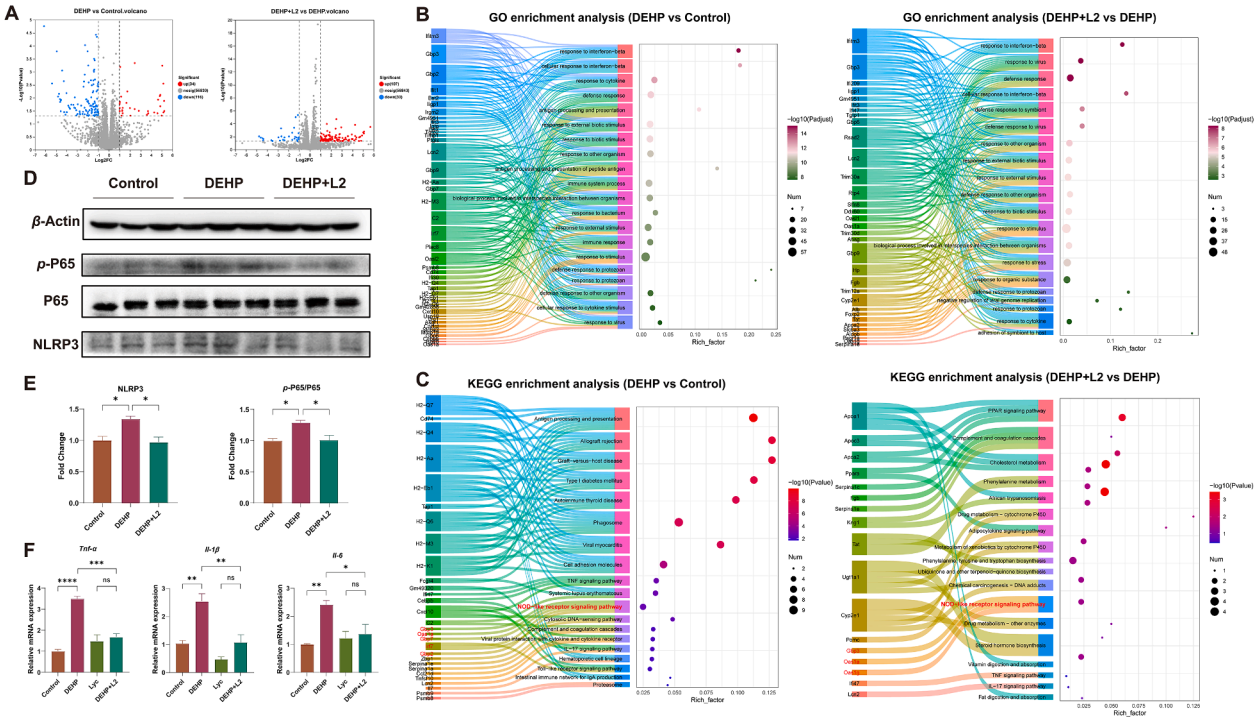

Fig. 2. Mechanism of Lyc transcriptome data analysis in DEHP-induced neurotoxicity. (A) Volcano plot (Fold change ≥ 2, P value < 0.05). (B) Sankey plot showcasing GO enrichment terms of DEGs in the DEHP vs Control and DEHP+Lyc vs DEHP comparisons. Dots of different sizes represent the numbers of enriched DEGs in distinct pathways. The data were analyzed via the online tool of the Majorbio Cloud Platform (https://cloud.majorbio.com/page/tools/). (C) Sankey plot showcasing KEGG enrichment analysis of DEGs in the DEHP vs Control and DEHP+Lyc vs DEHP groups. Dots of different sizes represent the numbers of enriched DEGs in distinct pathways. The data were analyzed via the online tool of the Majorbio Cloud Platform (https://cloud.majorbio.com/page/tools/). (D-E) Western blotting showing *p*-P65, P65, NLRP3, and *β*-Actin protein expression in the hippocampus. $n = 3$ per group. (F) The relative mRNA expression levels of *Tnf-α*, *Il-1β*, and *Il-6* in the hippocampus. $n = 3$ per group. The data represent the mean ± SEM and were analyzed using one-way ANOVA (Tukey post hoc test), and statistical significance was determined by $P < 0.05$. *$P < 0.05$, **$P < 0.01$, ***$P < 0.001$, ****$P < 0.0001$ and ns, not statistically significant.

demonstrate that DEHP exposure triggers anxiety- and depression-like behaviors, alongside increased systemic inflammation and oxidative stress, effects that Lyc (5 and 10 mg/kg) and Flu effectively alleviate.

Hippocampal transcriptomic analysis implicates the NOD-like receptor signaling pathway in DEHP-induced neurotoxicity and the protective effects of Lyc

To elucidate the molecular mechanisms underlying DEHP-induced neurotoxicity and Lyc's neuroprotective actions, we performed high-throughput RNA sequencing on hippocampal tissues from the Control, DEHP, and DEHP+L2 groups. RNA-seq data were validated by RT-qPCR for three randomly selected genes: *Lhfpl1, Lcor*, and *Tdrd1*. DEHP exposure upregulated the expression of these genes, an effect reversed by Lyc treatment, consistent with the RNA-seq results (Fig. S3A-B). While the Lyc-only group was not subjected to RNA-seq, RT-qPCR analysis showed no significant difference in *Lhfpl1, Lcor*, or *Tdrd1* expression compared to the control group (Fig. S3B). Principal component analysis (PCA) clearly demonstrated distinct clustering patterns among the experimental groups (Fig. S3C).

Volcano plot analysis identified 150 DEGs when comparing the DEHP group to the control group (34 upregulated, 116 downregulated), and 137 DEGs in the DEHP+Lyc group compared to the DEHP group (107 upregulated, 30 downregulated) (Fig. 2A). A hierarchical clustering heatmap visually represented the expression patterns of these DEGs (Fig. S3D). Gene Ontology (GO) enrichment analysis showed significant enrichment in immune response-related terms, including "response to interferon-beta", "defense response", "response to cytokine", "biological process involved in interspecies interaction between organisms", and "response to virus/defense response to virus", in both the DEHP vs. Control and DEHP+Lyc vs. DEHP comparisons (Fig. 2B). Kyoto Encyclopedia of Genes and Genomes (KEGG) pathway analysis further highlighted the enrichment of DEGs in inflammatory pathways (Fig. 2C). Several genes within the NOD-like receptor signaling pathway, including *Gbp3, Oas1a, Gbp7, Irf7, Gbp2*, and *Oas1g*, were identified as differentially expressed (Fig. 2C). While these genes are known for their roles in host defense, they have also been implicated in disease pathogenesis; for example, *Gbp3* is related to the development of lupus nephritis (Zhang et al., 2023), and *Oas1a* to Alzheimer's disease (Salih et al., 2019). However, these genes have not been observed before in DEHP or Lyc studies. Future experiments should aim to unravel the mechanisms of these genes in DEHP and Lyc.

Given the prominent involvement of the NOD-like receptor signaling pathway identified by transcriptomic analysis (Fig. 2C) and its reported association with DEHP-induced damage in other contexts (Dai et al., 2021; Li et al., 2023), we further investigated this pathway via western blotting. DEHP up-regulated the hippocampal NLRP3 and *p*-P65, while total P65 remained unchanged, leading to an elevated *p*-P65/P65 ratio (Fig. 2D-E). These findings imply activation of the NF-κB pathway downstream of NLRP3. Lyc treatment significantly reversed the increases in NLRP3, *p*-P65, and the *p*-P65/P65 ratio (Fig. 2D-E). Consistent with these protein findings, DEHP exposure in the hippocampus led to elevated mRNA expression of downstream proinflammatory cytokines *Tnf-α, Il-1β*, and *Il-6*, which can be reversed by Lyc treatment (Fig. 2F). Collectively, these data implicate the NOD-like receptor pathway in DEHP-induced neurotoxicity and suggest that Lyc exerts its neuroprotective effects, at least in part, by suppressing this pathway.

Lyc ameliorates DEHP-induced gut microbiota dysbiosis

Alpha diversity analysis showed no significant differences in the ACE, Sobs, Chao, and Coverage indices among groups (Fig. S4A). However, DEHP exposure significantly reduced the Shannon index and increased the Simpson index, indicating decreased community diversity. Lyc treatment did not significantly reverse these alpha diversity changes (Fig. 3A). Beta diversity analysis, including hierarchical clustering

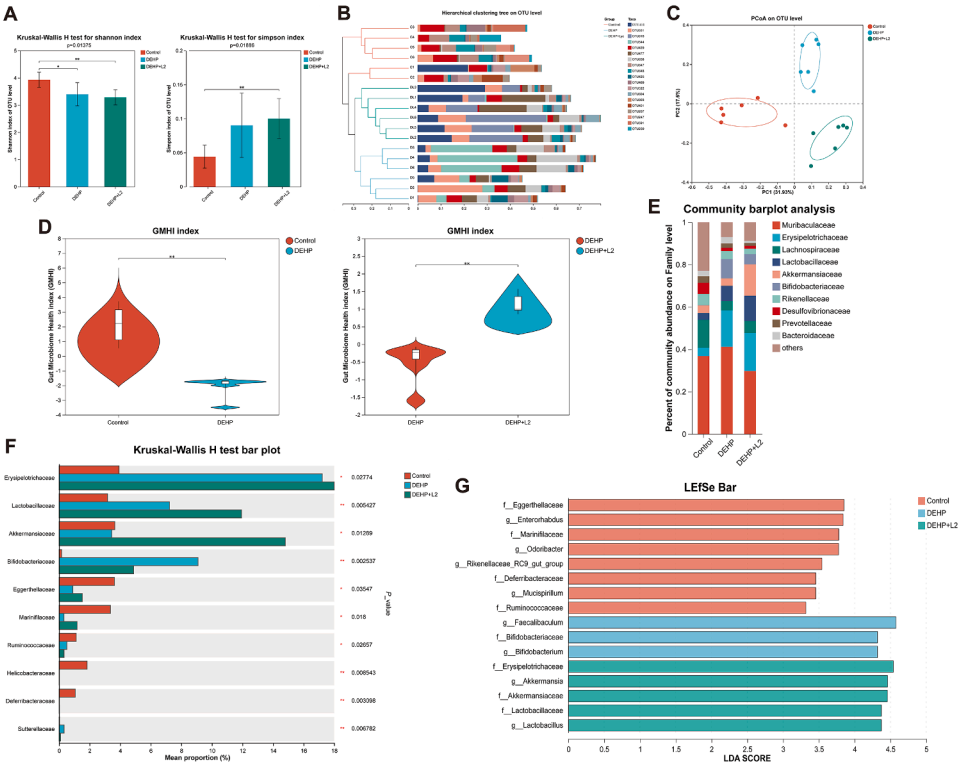

Fig. 3. Lyc effectively enhanced the composition of the gut microbiota. (A) Alpha diversity of the Shannon and Simpson indices (Kruskal-Wallis test). $n = 6$ per group. (B) Hierarchical clustering tree using bray_curtis at the OTU level. $n = 6$ per group. (C) PCoA using bray_curtis at the OTU level. $n = 6$ per group. (D) GMHI (Wilcoxon rank-sum test). $n = 6$ per group. (E) Bacterial community bar plot analysis at the family level (sum value). (F) Bacterial composition comparisons at the family level (Kruskal-Wallis H test). (G) LEfSe bar from family to genus (LDA value ≥ 3, all-against-all).

(Fig. 3B) and principal coordinate analysis (PCoA) (Fig. 3C), showed distinct clustering patterns between the Control, DEHP, and DEHP+Lyc groups, suggesting alterations in overall community composition. DEHP exposure significantly decreased the gut microbiome health index (GMHI) (Gupta et al., 2020), a measure of gut microbiome health, while Lyc treatment effectively restored the GMHI (Fig. 3D). Similarly, the microbial dysbiosis index (MDI) was elevated in the DEHP group and attenuated by Lyc treatment (Fig. S4B). Our findings suggest that Lyc promotes gut homeostasis by mitigating DEHP-induced dysbiosis.

Our study identified *Muribaculaceae, Erysipelotrichaceae, Lachnospiraceae, Lactobacillaceae, Akkermansiaceae*, and *Bifidobacteriaceae* as the predominant families (Fig. 3E). Phylum- and genus-level distributions are presented in Fig. S4C. DEHP exposure significantly decreased the relative abundance of *Verrucomicrobiota* at the phylum level and *Akkermansiaceae, Eggerthellaceae*, and *Marinifilaceae* at the family level, but increased the relative abundances of *Cyanobacteria* (phylum) and *Bacteroidaceae* (family) (Fig. S4D, Fig. 3F). At the genus level, DEHP exposure reseulte in increasing relative abundances of *Bifidobacterium* and *Faecalibaculum* while decreasing those of *Akkermansia, Enterorhabdus*, and *Odoribacter* (Fig. S4D). Lyc treatment largely reversed these DEHP-induced changes in microbial composition. Linear discriminant analysis Effect Size (LEfSe) analysis identified *Bifidobacteriaceae* as a potential key player in DEHP-induced neurotoxicity (Fig. 3G). While *Bifidobacteriaceae* are generally considered beneficial probiotics, their abundance was reported to increase following methamphetamine exposure in our previous work (Chen et al., 2021). Interestingly, *Bifidobacterium* species promote autophagy in intestinal epithelial cells (Lin et al., 2014). Lyc treatment enriched *Akkermansiaceae* and *Lactobacillaceae* (Fig. 3G), suggesting that Lyc's protective effects in this context may be mediated by the promotion of these beneficial families rather than by *Bifidobacteriaceae*. Recent studies have shown that Akkermansia muciniphila, a probiotic, improves cognitive dysfunction by regulating the BDNF and serotonin pathways in the gut-liver-brain axis (Kang et al., 2024), suggesting that it can ameliorate behavioral abnormalities and play an important role in neurological diseases. The initial discovery showed that *A. muciniphila Muc*^{T} can improve gut barrier function by restoring both the mucus layer thickness and the intestinal expression of the antimicrobial peptide Reg3g in mice (Everard et al., 2013). Our findings indicate that Lyc ameliorates DEHP-induced gut dysbiosis by restoring the balance of key bacterial families, particularly by increasing the abundance of *Akkermansiaceae* and *Lactobacillaceae*.

Lyc protects against DEHP-induced intestinal barrier dysfunction and colon inflammation by suppressing the LPS-TLR4/MyD88 pathway

Colon tissue morphology was then examined via H&E staining. Although no significant pathological alterations were observed

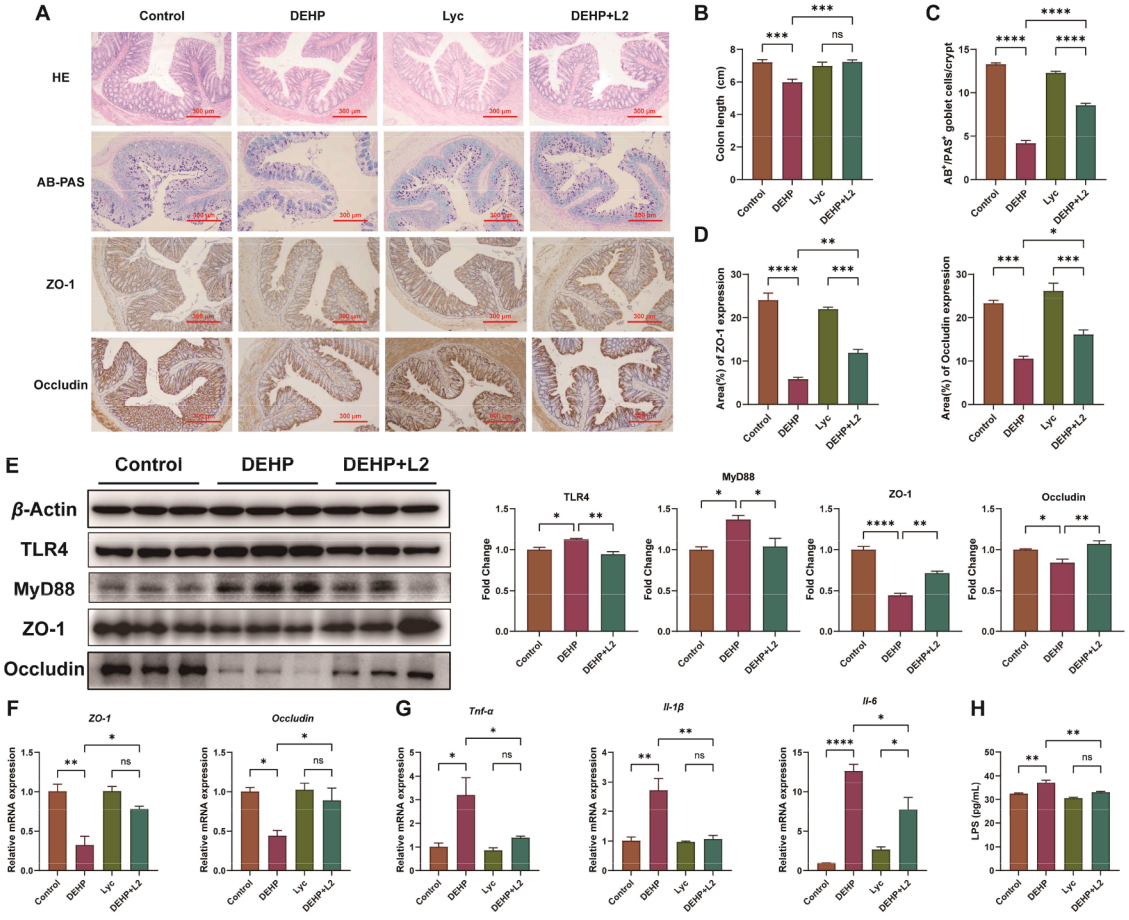

Fig. 4. Effects of Lyc on intestinal barrier impairment and colon inflammation. (A) H&E and AB-PAS staining and IHC of ZO-1 and Occludin (scale bar = 300 μm). (B) Length of the colon. $n = 6$ per group. (C) Quantification of AB/PAS-positive goblet cells per crypt. $n = 3$ per group. (D) Area (%) of ZO-1 and Occludin expression in the colon, as determined by IHC. $n = 3$ per group. (E) Western blotting showing TLR4, MyD88, ZO-1, Occludin and *β*-Actin protein expression in the colon. $n = 3$ per group. (F) The relative mRNA expression levels of *ZO-1* and *Occludin* in the colon. $n = 3$ per group. (G) The relative mRNA expression levels of *Tnf-α, Il-1β*, and *Il-6* in the colon. $n = 3$ per group. (H) Serum levels of LPS. $n = 4$ per group. The data represent the mean ± SEM and were analyzed using one-way ANOVA (Tukey post hoc test), and statistical significance was determined by $P < 0.05$. $^{*}P < 0.05$, $^{**}P < 0.01$, $^{***}P < 0.001$, $^{****}P < 0.0001$ and ns, not statistically significant.

(Fig. 4A), DEHP exposure significantly reduced colon length, an effect reversed by Lyc treatment (Fig. 4B). To further investigate barrier function, we evaluated the number of goblet cells as well as the tight junction proteins ZO-1 and Occludin. Compared with the control group, AB-PAS staining showed a decline in the number of goblet cells in the DEHP group, which Lyc treatment restored (Fig. 4A, C). IHC staining, western blotting, and RT-qPCR consistently demonstrated that DEHP exposure reduced the tight junction proteins, whereas Lyc treatment significantly reversed this effect (Fig. 4A and D–F).

Lipopolysaccharide (LPS) is a potent proinflammatory molecule contributing to systemic inflammation (Cao et al., 2018). LPS activates the TLR4/MyD88 signaling pathway, triggering downstream inflammatory responses (Di Vincenzo et al., 2024). In this study, we explored the effects of DEHP and Lyc on this pathway. Western blotting analysis revealed that DEHP exposure up-regulated TLR4 and MyD88 protein expression in the colon, an effect attenuated by Lyc treatment (Fig. 4E). Additionally, DEHP exposure significantly increased the mRNA expression of the downstream inflammatory cytokines *Tnf-α, Il-1β*, and *Il-6* in the colon, which was significantly reduced by Lyc treatment (Fig. 4G). We then measured serum LPS levels as an indicator of gut permeability and found that DEHP exposure up-regulated serum LPS, an effect significantly mitigated by Lyc treatment (Fig. 4H). The data indicate that Lyc reduced DEHP-induced intestinal barrier disruption and enteritis by interfering with the LPS-TLR4/MyD88 signaling pathway.

FMT from Lyc mice alleviates DEHP-induced anxiety-like and depression-like behavior, neuroinflammation and oxidative stress

Bacteriotherapy (FMT-L2) was employed to further investigate the crucial role of gut microbiota in the adverse effects of DEHP (Fig. 5A). In comparison to the DEHP group, the FMT-L2 intervention group displayed a significantly greatertotal distance traveled, entries into the center zone, and time spent in the center zone during the OFT (Fig. 5B-C), increased by 63 %, 118 %, and 46.6 %, respectively. FMT-L2 pretreatment led to a decrease in the entries into and time spent in the closed arms observed in DEHP-treated mice during the EPM (Fig. 5D-E), decreased by 29.3 % and 20.4 %, respectively. The results from the TST and FST confirmed the antidepressant effects of transplanting gut microbiota from Lyc-treated mice, as they demonstrated a reduction in immobility time relative to the DEHP group (Fig. 5F-G), decreased by 18.4 % and 23.4 %, respectively. Compared with the DEHP group, hippocampal neuronal damage was ameliorated by the FMT-L2 intervention, evidenced by decreased nuclear pyknosis in the CA1, CA3, and DG zones of the hippocampus (Fig. S5A). Following FMT-L2 intervention, inflammatory responses and oxidative stress were alleviated, as shown by decreased serum levels of TNF-*α*, IL-1*β*, IL-6, MDA, and ROS (Fig. 5H-I). These results revealed that the gut microbiome from Lyc has the same relieving effect as Lyc on DEHP-induced nervous system dysfunction.

Collectively, this study combined the application of behavioral, transcriptomic, molecular, microbiota, and bacteriotherapy analyses, and emphasizes the evidence for Lyc's protective role in DEHP-induced neurotoxicity at multiple levels. These findings strongly suggest that Lyc exert neuroprotective effects against neurotoxicity caused by DEHP by employing a comprehensive approach that includes adjusting the gut-brain axis, reducing neuroinflammation, and restoring gut balance.

Discussion

The widespread use of plastics and the resultant DEHP exposure present substantial health risks (Chao et al., 2015). The present study explored the involvement of the gut microbiota in neurotoxicity induced by DEHP and assessed the protective effects of Lyc. Through a comprehensive multi-omics approach and biochemical analyses, our findings revealed that DEHP exposure induced anxiety- and depression-like behaviors in mice. These behavioral alterations were

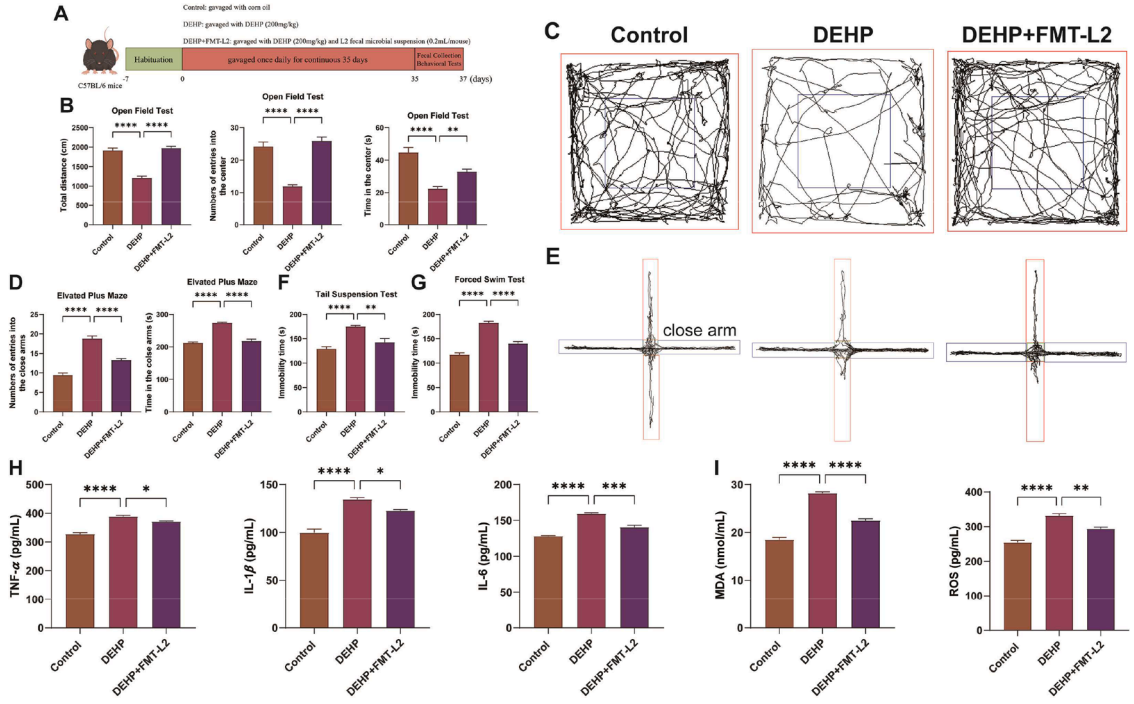

Fig. 5. Effects of gut microbiota from Lyc (5 mg/kg) on DEHP-induced abnormal behavior, neuroinflammation and oxidative stres. (A) Experimental period schematic diagram (By Figdraw. https://www.figdraw.com). (B) OFT: total distance, numbers of entries into the center and time in the center. $n = 10$ per group. (C) Trace representation of the OFT; (D) EPM: numbers of entries into the close arms and time in the close arms. $n = 10$ per group. (E) Representative tracks of the EPM; (F, G) Duration of immobility in the TST (F) and FST (G). $n = 6$–8 per group. (H, I) Serum levels of inflammatory cytokines (TNF-*α*, IL-1*β*, and IL-6) and oxidative stress markers (MDA and ROS). $n = 4$ per group. The data represent the mean ± SEM and were analyzed using one-way ANOVA (Tukey post hoc test), and statistical significance was determined by $P < 0.05$. *$P < 0.05$, **$P < 0.01$, ***$P < 0.001$, ****$P < 0.0001$ and ns, not statistically significant.

related to heightened inflammatory responses in the hippocampus. Furthermore, DEHP exposure significantly altered gut microbiota composition and compromised intestinal barrier integrity. Notably, Lyc treatment effectively counteracted these adverse effects by alleviating anxiety- and depression-like behaviors and attenuating neuroinflammation in the hippocampus, potentially through modulation of the NOD-like receptor signaling pathway. Moreover, Lyc restored gut microbiota homeostasis and enhanced intestinal barrier function, possibly through modulation of the LPS-TLR4/MyD88 pathway. In the present research, we elucidated that Lyc ameliorates DEHP-induced neurotoxicity through the gut-brain axis in mice (Fig. 6). These findings propose a novel therapeutic strategy for DEHP-induced neurotoxicity by targeting this crucial axis.

Our results support earlier investigations linking DEHP exposure to neurotoxicity and neurobehavioral deficits (Yang et al., 2023), such as DEHP exposure induces anxiety- and depression-like behaviors in mice (Kang et al., 2021; Kang et al., 2023). In addition, previous studies have shown that DEHP resulted in neurotoxicity and behavioral abnormalities via upregulating the expression of oxidative stress-associated proteins (Mo et al., 2024; Tang et al., 2023). Integrating our findings with the existing literature, we propose that DEHP contributes to behavioral abnormalities through enhanced neuroinflammation, systemic inflammation, and oxidative stress. These findings underscore Lyc's potential in mitigating DEHP-associated health risks. The NOD-like receptor (NLR) family plays a critical role in initiating innate immune responses to cellular injury and stress (Platnich and Muruve, 2019). Specifically, NLRP3 induces inflammation through NF-κB signaling pathway activation or promotion of oxidative stress (Jo et al., 2016). Recent research has demonstrated that phenolamide methyl (3,4,5-trimethoxybenzoyl) alanate mitigates DEHP-induced inflammation by modulating the NLRP3 and NF-κB signaling pathways (Bu et al., 2024). Previous study findings may provide new evidence that Lyc alleviates cognitive impairment caused by paclitaxel in mice by counteracting oxidative stress, endoplasmic reticulum stress, and inflammation through the reduction of the levels of the NLRP3 inflammasome (Zakaria et al., 2025). Similar to previous studies, the findings of our study revealed that Lyc may ameliorate behavioral issues, neuroinflammation, and oxidative stress by regulating the NLRP3 and NF-κB pathways, as evidenced by RNA sequencing and western blotting analyses.

The gut-brain axis, encompassing neural, endocrine, and inflammatory routes, can be disrupted, potentially leading to various neurodevelopmental disorders (Osadchiy et al., 2019). Altered gut-derived signaling molecules influence brain function, behavior, and cognition through neural pathways, endocrine signaling mechanisms, and immune system modulation (Westfall et al., 2017). Our findings suggested that the intestinal flora of DEHP-induced anxiety and depression model mice was significantly altered compared with control mice. Various unhealthy phenotypes have been associated with lower GMHI (Li et al., 2023) and higher MDI (Xu et al., 2020). In our study, we observed that Lyc administration significantly elevated the relative abundance of *Akkermansiaceae, Marinifilaceae*, and *Odoribacter*, which were decreased in DEHP-treated mice. Recent studies have linked *Marinifilaceae* and *Akkermansiaceae* to alterations in gut, serum, brain, and lipid metabolites in APP/PS1 mice, suggesting potential therapeutic targets for Alzheimer's disease (Cheng et al., 2022). *Marinifilaceae*, a member of the *Bacteroidetes* phylum, is inversely correlated with proinflammatory cytokines (Kim et al., 2019). *Akkermansia* acts as a crucial health regulator, beneficially influencing metabolic disorders, neurodegenerative conditions, cancer, immune function, and intestinal barrier maintenance (Panzetta and Valdivia, 2024; Sun et al., 2023). When *Akkermansia* colonizes the intestinal mucosal layer, its increased abundance can enhance intestinal mucins, strengthening the intestinal chemical barrier (Paone and Cani, 2020). *Akkermansia muciniphila*, a known probiotic in the gut microbiome, has demonstrated the ability to rebalance gut microbiota, repair the intestinal mucosal barrier, and modulate host immune responses and neuroinflammation via short chain fatty acids (Cani et al., 2022), hence diminishing neural damage and behavioral disturbances in various ailments (Zhu et al., 2025). *Akkermansia muciniphila* alleviated the anxiety phenotype by restoring the imbalance of tryptophan metabolism and increasing 5-HT activity (Pan et al., 2025). Thus, we speculated that the increased abundance of *Akkermansiaceae*, which produces short chain fatty acids or neurotransmitter, contributed to the improvement of Lyc on nervous system and intestinal injury.

While H&E staining of the colon revealed no significant pathological changes, DEHP significantly compromised intestinal barrier integrity, and Lyc helped protect against this DEHP-induced weakening. This included a decrease in the number of goblet cells and reduced expression of the tight junction proteins ZO-1 and Occludin in the DEHP group. It is plausible that chronic inflammation or alterations in gut homeostasis associated with this compromised barrier integrity, even if not manifesting as gross histological lesions on H&E, could contribute to changes in colon morphology, such as the observed reduction in length. Epithelial tight junctions, primarily composed of ZO-1 and occludin, are vital for maintaining intestinal barrier integrity, regulating nutrient

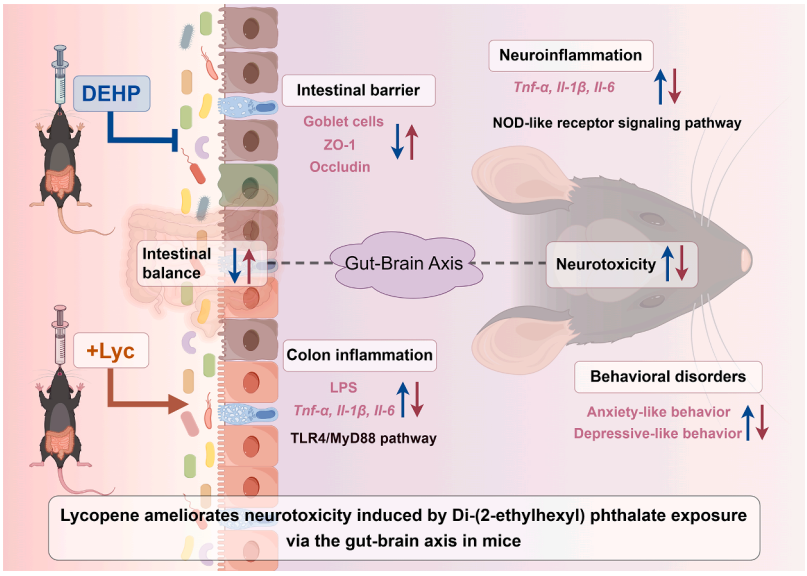

Fig. 6. Mechanism by which Lyc prevents DEHP-induced neurotoxicity via the gut-brain axis in mice.

absorption while restricting bacterial adhesion (Lee et al., 2018). Intestinal barriers are crucial in protecting against external toxic and pathogenic stimuli (Macura et al., 2024). LPS, a key inflammatory trigger, initiates inflammatory cytokine release through TLR4 activation and compromises the intestinal barrier (Wang et al., 2011). Lyc has the potential to reduce intestinal permeability and blood LPS levels, which in turn inhibits the cardiovascular TLR4 signaling cascade and prevents the progression of atherosclerosis (Tu et al., 2023). Our results revealed that DEHP significantly elevated TLR4 expression in the colon and plasma LPS levels, an effect attenuated by Lyc treatment. Moreover, Lyc enhanced tight junction protein expression and reduced gut permeability, suggesting its protective role against DEHP-induced intestinal barrier dysfunction through the LPS-TLR4/MyD88 pathway. Nevertheless, gene knockdown studies are required to confirm the causal role of particular components within the LPS-TLR4/MyD88 signalling cascade.

Intestinal microbiota disorders are directly linked to central nervous system diseases, highlighting the important role of the intestinal microbiota. We conducted an intervention experiment using fecal microbiota from Lyc-treated mice. Studies have shown that intestinal microbiota from healthy mice can enhance spinal cord injury recovery (Jing et al., 2021), and alleviate impairments in cognitive function and depression-associated behaviors (Xiao et al., 2022). In this study, FMT from Lyc-treated mice mitigated the adverse effects of DEHP, suggesting that the gut microbiome is associated with DEHP-mediated neurotoxicity and holds significant potential for reversing DEHP-induced neurotoxicity. Collectively, the results from the FMT experiments using gut microbiota from Lyc-treated mice demonstrated that Lyc improves DEHP-induced neurotoxicity through the gut-brain axis.

This research integrated 3 key technical systems: transcriptome, microbiome and molecular biology, offering a novel approach to understanding how Lyc counteracts DEHP-induced neurotoxicity. By analyzing the brain's transcriptome, changes in the crucial KEGG pathways-NOD-like receptor signaling pathway associated with Lcy's mitigation of DEHP-induced neurotoxicity were identified. The mechanisms regulating important targets and pathways at the gene and protein levels are verified by molecular biotechnology. Furthermore, through microbiome analysis, the changes in the composition of the gut microbiota were clarified, and the key microbiota, *Akkermansiaceae*, may be the beneficial bacterial taxa mediating the effects of Lcy on mitigating DEHP-induced neurotoxicity. The findings of the study highlight the growing concern over environmental pollutants such as DEHP and their impact on neurological and gastrointestinal health.

Several limitations should be acknowledged in this study. While our findings suggest that Lyc ameliorates DEHP-induced neurotoxicity potentially by modulating the NOD-like receptor signaling pathway, restoring gut microbiota balance, enhancing intestinal barrier function, and curbing colonic inflammation via the LPS-TLR4/MyD88 signaling pathway, we did not perform western blot validation of these specific protein pathways in the Lyc-only treatment group. Based on preliminary observations, this decision was made as both phenotypic data (Fig. 1) and RT-qPCR results for selected genes (Figure S3B, used to validate RNA-seq findings) indicated no significant differences between the Lyc-only treated group and the control. Consequently, RNA-seq and further western blot experiments for these pathways were not pursued for the Lyc-only group, allowing a focused investigation of the interaction effects between DEHP and Lyc. Furthermore, relying solely on male mice restricts the applicability of these results to both genders, highlighting the necessity for gender-inclusive research to comprehensively evaluate Lyc's therapeutic potential. In addition, clinical data were not incorporated in this research, so the results of this study do not address the generalisability of mouse data to humans. Subsequent studies can utilize different gender animal models and include clinical data to enhance the reliability of the research results.

Conclusions

Given the substantial health risks posed by DEHP, developing effective preventive strategies is crucial. This study provides compelling evidence that Lyc positively modulates brain function, gut microbiota composition, and intestinal barrier integrity in DEHP-treated mice. Lyc exerts neuroprotective effects against DEHP exposure by modulating the NOD-like receptor signaling pathway. Furthermore, Lyc effectively restores gut microbiota balance, enhances intestinal barrier function, and suppresses inflammation through the LPS-TLR4/MyD88 signaling pathway. These findings establish a foundation for understanding Lyc's therapeutic potential in treating DEHP-induced neurotoxicity through the microbiota-gut-brain axis and suggest novel applications for Lyc in managing DEHP-related conditions. These findings highlight Lyc's therapeutic potential in mitigating DEHP-induced neurotoxicity via the microbiota-gut-brain axis and propose its application as a novel dietary strategy for managing DEHP-related neurological disorders. Although these findings are based on a murine model, they offer valuable insights into potential translational applications of Lycopene as a dietary intervention for individuals at risk of environmental toxin exposure. Further studies, including clinical trials and mechanistic validation in human models, are warranted to confirm the generalizability of these results.

Author statement

All the data were generated in-house, and no paper mill was used. All authors agree to be accountable for all aspects of work ensuring integrity and accuracy.

Funding

This work was supported by the National Natural Science Foundation of China (Grant Nos. 82171877, 82173474 and 82471914) and the Guangdong Natural Science Foundation (Grant Nos. 2023A1515012476 and 2024A1515010708).

Data availability

All of the RNA-seq datasets of the hippocampus were submitted to the Sequence Read Archive of the National Center for Biotechnology Information under the accession number PRJNA11175609. Additionally, the 16S rRNA sequencing datasets for fecal bacteria have been deposited in the NCBI Sequence Read Archive with accession number PRJNA 1181227.

CRediT authorship contribution statement

Li-Jian Chen: Writing – original draft, Project administration, Conceptualization. **Yi Liu:** Writing – original draft, Project administration, Data curation. **Jia-Li Liu:** Writing – original draft, Project administration, Formal analysis. **Zhi-Jiang Chen:** Methodology, Investigation. **Wei Zhao:** Software, Resources. **Ji-Hui Li:** Visualization, Validation. **Clare Hsu:** Visualization, Data curation. **Long Chen:** Validation, Formal analysis. **Jia-Hao Zeng:** Supervision, Investigation. **Xiu-Wen Li:** Software, Methodology. **Jian-Zheng Yang:** Software, Resources. **Jia-Hao Li:** Software, Resources. **Xiao-Li Xie:** Supervision, Conceptualization. **Shao-Hua Tao:** Writing – review & editing, Supervision. **Qi Wang:** Writing – review & editing, Supervision, Funding acquisition, Conceptualization.

Declaration of competing interest

The authors declare that they have no known competing financial interests or personal relationships that could have appeared to influence the work reported in this paper.

Acknowledgments

During the preparation of this work, the authors used Home for Researchers (https://www.home-for-researchers.com/) and American Journal Experts' AI writing assistant, Curie (https://www.aje.cn/curie/), for English language editing. After using these services, the authors reviewed and edited the content as necessary and take full responsibility for the publication's content.

Supplementary materials

Supplementary material associated with this article can be found, in the online version, at doi:10.1016/j.phymed.2025.157057.

Supplementary Figure 1. (A) Chemical structure of DEHP. (B) Chemical structure of Lyc. (C) Chemical structure of Flu.

Supplementary Figure 2. (A) Hippocampal morphological changes, including those in the CA1, CA3, and DG regions, were observed via HE staining (scale bar = 400 μm). (B) Examination of the correlations between inflammatory cytokines and oxidative stress markers. The correlation was determined via Pearson's correlation coefficient. The correlation analysis was performed using the OmicStudio tools at https://www.omicstudio.cn/tool.

Supplementary Figure 3. Results of the RNA-seq data. (A) RNA-seq expression of *Lhfpl1, Lcor*, and *Tdrd1*. (B) RT-qPCR verification of *Lhfpl1, Lcor*, and *Tdrd1*. (C) PCA of the RNA-seq data. (D) Hierarchical clustering of the DEGs in the hippocampus. The blue color indicates genes whose expression was downregulated, and the red color indicates genes whose expression was upregulated. The data represent the mean ± SEM and were analyzed using one-way ANOVA (Tukey post hoc test), and statistical significance was determined by $P < 0.05$. $^{*}P < 0.05$, $^{**}P < 0.01$, $^{***}P < 0.001$, $^{****}P < 0.0001$ and ns, not statistically significant.

Supplementary Figure 4. The diversity and composition of the gut microbiota in different groups. (A) Alpha diversity of the Ace, Sobs, Chao, and Coverage indices (Kruskal-Wallis test). $n = 6$ per group. (B) MDI (Wilcoxon rank-sum test). $n = 6$ per group. (C) Bacterial community bar plot analysis at the phylum and genus levels (sum value). (D) Bacterial composition comparisons at the phylum and genus levels (Kruskal-Wallis H test).

Supplementary Figure 5. (A) Hippocampal morphological changes, including those in the CA1, CA3, and DG regions, were observed via HE staining (scale bar = 400 μm).

References

Beheshti, F., Hashemzehi, M., Hosseini, M., Marefati, N., Memarpour, S., 2020. Inducible nitric oxide synthase plays a role in depression- and anxiety-like behaviors chronically induced by lipopolysaccharide in rats: evidence from inflammation and oxidative stress. Behav. Brain Res. 392, 112720.

Bu, F., Zheng, M., Li, N., Yan, X., Xin, H., Li, Y., Zhang, F., 2024. Portulaca oleracea L. Phenolic amide methyl (3,4,5-Trimethoxybenzoyl) valylprolinate attenuates diethylhexyl phthalate-induced Human umbilical vein endothelial cells' Inflammation through NLRP3 and NF-κb pathways. J. Med. Food 27, 971–980.

Cani, P.D., Depommier, C., Derrien, M., Everard, A., de Vos, W.M., 2022. Akkermansia muciniphila: paradigm for next-generation beneficial microorganisms. Nat. Rev. Gastro. Hepat. 19, 625–637.

Cao, S., Zhang, Q., Wang, C., Wu, H., Jiao, L., Hong, Q., Hu, C., 2018. LPS challenge increased intestinal permeability, disrupted mitochondrial function and triggered mitophagy of piglets. Innate. Immun-London 24, 221–230.

Chao, K., Huang, C., Wei, C., 2015. Health risk assessments of DEHP released from chemical protective gloves. J. Hazard. Mater. 283, 53–59.

Chen, L., Zhi, X., Zhang, K., Wang, L., Li, J., Liu, J., Xu, L., Yoshida, J.S., Xie, X., Wang, Q., 2021. Escalating dose-multiple binge methamphetamine treatment elicits neurotoxicity, altering gut microbiota and fecal metabolites in mice. Food Chem. Toxicol. 148, 111946.

Cheng, X., Tan, Y., Li, H., Huang, J., Zhao, D., Zhang, Z., Yi, M., Zhu, L., Hui, S., Yang, J., Peng, W., 2022. Fecal 16S rRNA sequencing and multi-compartment metabolomics revealed gut microbiota and metabolites interactions in APP/PS1 mice. Comput. Biol. Med. 151, 106312.

Cryan, J.F., Dinan, T.G., 2012. Mind-altering microorganisms: the impact of the gut microbiota on brain and behaviour. Nat. Rev. Neurosci. 13, 701–712.

Cui, J.G., Zhao, Y., Zhang, H., Li, X.N., Li, J.L., 2022. Lycopene regulates the mitochondrial unfolded protein response to prevent DEHP-induced cardiac mitochondrial damage in mice. Food Funct. 13, 4527–4536.

Dai, X., Li, X., Zhu, S., Li, M., Zhao, Y., Talukder, M., Li, Y., Li, J., 2021. Lycopene ameliorates Di(2-ethylhexyl) phthalate-induced pyroptosis in spleen via suppression of classic caspase-1/NLRP3 pathway. J. Agr. Food Chem. 69, 1291–1299.

Dai, X.Y., Zhu, S.Y., Chen, J., Li, M.Z., Talukder, M., Li, J.L., 2022. Role of toll-like receptor/MyD88 signaling in lycopene alleviated di-2-ethylhexyl phthalate (DEHP)-induced inflammatory response. J. Agr. Food Chem. 70, 10022–10030.

Di Vincenzo, F., Del Gaudio, A., Petito, V., Lopetuso, L.R., Scaldaferri, F., 2024. Gut microbiota, intestinal permeability, and systemic inflammation: a narrative review. Intern. Emerg. Med. 19, 275–293.

Erythropel, H.C., Maric, M., Nicell, J.A., Leask, R.L., Yargeau, V., 2014. Leaching of the plasticizer di(2-ethylhexyl)phthalate (DEHP) from plastic containers and the question of human exposure. Appl. Microbiol. Biot. 98, 9967–9981.

Everard, A., Belzer, C., Geurts, L., Ouwerkerk, J.P., Druart, C., Bindels, L.B., Guiot, Y., Derrien, M., Muccioli, G.G., Delzenne, N.M., de Vos, W.M., Cani, P.D., 2013. Cross-talk between*Akkermansia muciniphila* and intestinal epithelium controls diet-induced obesity. Proceed. National Acad. Sci. 110, 9066–9071.

Gao, X., Zhao, X., Liu, M., Zhao, H., Sun, Y., 2023. Lycopene prevents non-alcoholic fatty liver disease through regulating hepatic NF-kappaB/NLRP3 inflammasome pathway and intestinal microbiota in mice fed with high-fat and high-fructose diet. Front. Nutr. 10, 1120254.

Gupta, V.K., Kim, M., Bakshi, U., Cunningham, K.Y., Davis, J.M., Lazaridis, K.N., Nelson, H., Chia, N., Sung, J., 2020. A predictive index for health status using species-level gut microbiome profiling. Nat. Commun. 11.

He, L., Mo, X., He, L., Ma, Q., Cai, L., Zheng, Y., Huang, L., Lin, X., Wu, M., Ding, W., Zhou, C., Zhang, J., Hashimoto, K., Yao, W., Chen, J., 2024. The role of BDNF transcription in the antidepressant-like effects of 18β-glycyrrhetinic acid in a chronic social defeat stress model. Phytomedicine 132, 155332.

Imran, M., Ghorat, F., Ul-Haq, I., Ur-Rehman, H., Aslam, F., Heydari, M., Shariati, M.A., Okuskhanova, E., Yessimbekov, Z., Thiruvengadam, M., Hashempur, M.H., Rebezov, M., 2020. Lycopene as a natural antioxidant used to prevent Human health disorders. Antioxidants-Basel 9, 706.

Jing, Y., Yu, Y., Bai, F., Wang, L., Yang, D., Zhang, C., Qin, C., Yang, M., Zhang, D., Zhu, Y., Li, J., Chen, Z., 2021. Effect of fecal microbiota transplantation on neurological restoration in a spinal cord injury mouse model: involvement of brain-gut axis. Microbiome 9.

Jo, E., Kim, J.K., Shin, D., Sasakawa, C., 2016. Molecular mechanisms regulating NLRP3 inflammasome activation. Cell Mol. Immunol. 13, 148–159.

Kang, E.J., Cha, M., Kwon, G., Han, S.H., Yoon, S.J., Lee, S.K., Ahn, M.E., Won, S., Ahn, E. H., Suk, K.T., 2024. Akkermansia muciniphila improve cognitive dysfunction by regulating BDNF and serotonin pathway in gut-liver-brain axis. Microbiome 12, 181.

Kang, J.S., Baek, J.H., Jung, S., Chung, H.J., Lee, D.K., Kim, H.J., 2021a. Ingestion of Bis (2-ethylhexyl) phthalate (DEHP) during adolescence causes depressive-like behaviors through hypoactive glutamatergic signaling in the medial prefrontal cortex. Environ. Pollut. 289, 117978.

Kang, J.S., Baek, J.H., Jung, S., Chung, H.J., Lee, D.K., Kim, H.J., 2021b. Ingestion of Bis (2-ethylhexyl) phthalate (DEHP) during adolescence causes depressive-like behaviors through hypoactive glutamatergic signaling in the medial prefrontal cortex. Environ. Pollut. 289, 117978.

Kang, J.S., Baek, J.H., Song, M.Y., Rehman, N.U., Chung, H.J., Lee, D.K., Yoo, D.Y., Kim, H.J., 2023. Long-term exposure changes the environmentally relevant bis(2-ethylhexyl) phthalate to be a neuro-hazardous substance disrupting neural homeostasis in emotional and cognitive functions. Environ. Pollut. 324, 121387.

Kim, S.J., Kim, S., Kim, A., Kang, S., Park, M., Sung, M., 2019. Dietary fat intake and age modulate the composition of the gut microbiota and colonic inflammation in C57BL/6J mice. BMC. Microbiol. 19.

Lee, B., Moon, K.M., Kim, C.Y., 2018. Tight junction in the intestinal epithelium: its association with diseases and regulation by phytochemicals. J. Immunol. Res. 2018, 1–11.

Lei, M., Menon, R., Manteiga, S., Alden, N., Hunt, C., Alaniz, R.C., Lee, K., Jayaraman, A., Dorrestein, P.C., 2019. Environmental chemical diethylhexyl phthalate alters intestinal microbiota community structure and metabolite profile in mice. Msystems. 4.

Li, M., Zhao, Y., Dai, X., Talukder, M., Li, J., 2023a. Lycopene ameliorates DEHP exposure-induced renal pyroptosis through the Nrf2/Keap-1/NLRP3/caspase-1 axis. J. Nutr. Biochem. 113, 109266.

Li, M.Z., Zhao, Y., Dai, X.Y., Talukder, M., Li, J.L., 2023b. Lycopene ameliorates DEHP exposure-induced renal pyroptosis through the Nrf2/Keap-1/NLRP3/caspase-1 axis. J. Nutr. Biochem. 113, 109266.

Li, Y., Xie, G., Zha, Y., Ning, K., 2023c. GAN-GMHI: a generative adversarial network with high discriminative power for microbiome-based disease prediction. J. Genet. Genomics. 50, 1026–1028.

Lin, R., Jiang, Y., Zhao, X.Y., Guan, Y., Qian, W., Fu, X.C., Ren, H.Y., Hou, X.H., 2014. Four types of bifidobacteria trigger autophagy response in intestinal epithelial cells. J. Digest. Dis. 15, 597–605.

Long, Y., Paengkoum, S., Lu, S., Niu, X., Thongpea, S., Taethaisong, N., Han, Y., Paengkoum, P., 2024. Physicochemical properties, mechanism of action of lycopene and its application in poultry and ruminant production. Front. Vet. Sci. 11, 1364589.

Macura, B., Kiecka, A., Szczepanik, M., 2024. Intestinal permeability disturbances: causes, diseases and therapy. Clin. Exp. Med. 24.

Mo, H., Shan, C., Chen, L., Chen, X., Han, C., Wu, D., Tao, F., Gao, H., 2024. Antioxidant vitamins' modification of the adverse health effects induced by phthalate exposure: a scoping review of epidemiological and experimental studies. Ecotox. Environ. Safe. 286, 117190.

Osadchiy, V., Martin, C.R., Mayer, E.A., 2019. The gut–Brain axis and the microbiome: mechanisms and clinical implications. Clin. Gastroenterol. H 17, 322–332.
Ozkan, G., Günal-Köroğlu, D., Karadag, A., Capanoglu, E., Cardoso, S.M., Al-Omari, B., Calina, D., Sharifi-Rad, J., Cho, W.C., 2023. A mechanistic updated overview on lycopene as potential anticancer agent. Biomed. Pharmac Other 161, 114428.
Pan, M., Qian, C., Huo, S., Wu, Y., Zhao, X., Ying, Y., Wang, B., Yang, H., Yeerken, A., Wang, T., Fu, M., Wang, L., Wei, Y., Zhao, Y., Shao, C., Wang, H., Zhao, C., 2025. Gut-derived lactic acid enhances tryptophan to 5-hydroxytryptamine in regulation of anxiety via Akkermansia muciniphila. Gut. Microbes. 17, 2447834.
Panzetta, M.E., Valdivia, R.H., 2024. Akkermansia in the gastrointestinal tract as a modifier of human health. Gut. Microbes. 16, 2406379.
Paone, P., Cani, P.D., 2020. Mucus barrier, mucins and gut microbiota: the expected slimy partners? Gut 69, 2232–2243.
Patki, G., Solanki, N., Atrooz, F., Allam, F., Salim, S., 2013. Depression, anxiety-like behavior and memory impairment are associated with increased oxidative stress and inflammation in a rat model of social stress. Brain Res. 1539, 73–86.
Platnich, J.M., Muruve, D.A., 2019. NOD-like receptors and inflammasomes: a review of their canonical and non-canonical signaling pathways. Arch. Biochem. Biophys. 670, 4–14.
Salih, D.A., Bayram, S., Guelfi, S., Reynolds, R.H., Shoai, M., Ryten, M., Brenton, J.W., Zhang, D., Matarin, M., Botia, J.A., Shah, R., Brookes, K.J., Guetta-Baranes, T., Morgan, K., Bellou, E., Cummings, D.M., Escott-Price, V., Hardy, J., 2019. Genetic variability in response to amyloid beta deposition influences Alzheimer's disease risk. Brain Commun. 1.
Su, H., Yuan, P., Lei, H., Zhang, L., Deng, D., Zhang, L., Chen, X., 2022. Long-term chronic exposure to di-(2-ethylhexyl)-phthalate induces obesity via disruption of host lipid metabolism and gut microbiota in mice. Chemosphere 287, 132414.
Sun, Y., Zhu, H., Cheng, R., Tang, Z., Zhang, M., 2023. Outer membrane protein Amuc_1100 of Akkermansia muciniphila alleviates antibiotic-induced anxiety and depression-like behavior in mice. Physiol. Behav. 258, 114023.
Tang, S., Zhang, H., Xia, Y., Luo, S., Liu, Y., Duan, X., Zou, Z., Chen, C., Zhou, L., Qiu, J., 2023. Exposure to di (2-ethylhexyl) phthalate causes locomotor increase and anxiety-like behavior via induction of oxidative stress in brain. Toxicol. Mech. Method. 33, 113–122.
Tu, T., Liu, H., Liu, Z., Liang, Y., Tan, C., Feng, D., Zou, J., 2023. Amelioration of atherosclerosis by lycopene is linked to the modulation of gut microbiota dysbiosis and related gut-heart axis activation in high-fat diet-fed ApoE−/− mice. Nutr. Metab. 20, 53.
Wang, H., Li, M., Cui, J., Zhang, H., Zhao, Y., Li, J., 2023a. Lycopene prevents phthalate-induced cognitive impairment via modulating ferroptosis. J. Agr. Food Chem. 71, 16727–16738.
Wang, H.R., Li, M.Z., Cui, J.G., Zhang, H., Zhao, Y., Li, J.L., 2023b. Lycopene prevents phthalate-induced cognitive impairment via modulating ferroptosis. J. Agr. Food Chem. 71, 16727–16738.
Wang, J., Qiu, F., Zhang, Z., Liu, Y., Zhou, Q., Dai, S., Xiang, S., Wei, C., 2023c. *Clostridium butyricum* alleviates DEHP plasticizer-induced learning and memory impairment in mice via gut–Brain axis. J. Agr. Food. Chem. 71, 18524–18537.
Wang, J.X., Zhao, Y., Chen, M.S., Zhang, H., Cui, J.G., Li, J.L., 2023d. Heme-oxygenase-1 as a target for phthalate-induced cardiomyocytes ferroptosis. Environ. Pollut. 317, 120717.
Wang, M., Chen, Y., Zhang, Y., Zhang, L., Lu, X., Chen, Z., 2011. Mannan-binding lectin directly interacts with Toll-like receptor 4 and suppresses lipopolysaccharide-induced inflammatory cytokine secretion from THP-1 cells. Cell Mol. Immunol. 8, 265–275.
Wang, P., Ouyang, H., Bi, G., Liang, F., Hu, S., Wu, C., Jiang, X., Zhou, W., Li, D., Zhang, S., Yang, X., Zhao, M., Fang, J., Wang, H., Jia, W., Zhu, Z., Bi, H., 2025. Schisandrol B alleviates depression-like behavior in mice by regulating bile acid homeostasis in the brain-liver-gut axis via the pregnane X receptor. Phytomedicine 137, 156340.
Wang, R., Xu, X., Zhu, Q., 2016. Pubertal exposure to di-(2-ethylhexyl) phthalate influences social behavior and dopamine receptor D2 of adult female mice. Chemosphere 144, 1771–1779.
Westfall, S., Lomis, N., Kahouli, I., Dia, S.Y., Singh, S.P., Prakash, S., 2017. Microbiome, probiotics and neurodegenerative diseases: deciphering the gut brain axis. Cell Mol. Life Sci. 74, 3769–3787.
Wu, S.X., Li, J., Zhou, D.D., Xiong, R.G., Huang, S.Y., Saimaiti, A., Shang, A., Li, H.B., 2022a. Possible effects and mechanisms of dietary natural products and nutrients on depression and Anxiety: a narrative review. Antioxidants-Basel 11.
Wu, Y., Wang, J., Zhao, T., Chen, J., Kang, L., Wei, Y., Han, L., Shen, L., Long, C., Wu, S., Wei, G., 2022b. Di-(2-ethylhexyl) phthalate exposure leads to ferroptosis via the HIF-1α/HO-1 signaling pathway in mouse testes. J. Hazard. Mater. 426, 127807.
Xiao, W., Su, J., Gao, X., Yang, H., Weng, R., Ni, W., Gu, Y., 2022. The microbiota-gut-brain axis participates in chronic cerebral hypoperfusion by disrupting the metabolism of short-chain fatty acids. Microbiome 10.
Xu, R., Wu, B., Liang, J., He, F., Gu, W., Li, K., Luo, Y., Chen, J., Gao, Y., Wu, Z., Wang, Y., Zhou, W., Wang, M., 2020. Altered gut microbiota and mucosal immunity in patients with schizophrenia. Brain Behav. Immun. 85, 120–127.
Yang, L., Zou, J., Zang, Z., Wang, L., Du, Z., Zhang, D., Cai, Y., Li, M., Li, Q., Gao, J., Xu, H., Fan, X., 2023. Di-(2-ethylhexyl) phthalate exposure impairs cortical development in hESC-derived cerebral organoids. Sci. Total. Environ. 865, 161251.
Yang, Y., Sun, F., Chen, H., Tan, H., Yang, L., Zhang, L., Xie, J., Sun, J., Huang, X., Huang, Y., 2021. Postnatal exposure to DINP was associated with greater alterations of lipidomic markers for hepatic steatosis than DEHP in postweaning mice. Sci. Total. Environ. 758, 143631.
Yu, Z., Shi, Z., Zheng, Z., Han, J., Yang, W., Lu, R., Lin, W., Zheng, Y., Nie, D., Chen, G., 2021. DEHP induce cholesterol imbalance via disturbing bile acid metabolism by altering the composition of gut microbiota in rats. Chemosphere 263, 127959.
Zakaria, N., Menze, E.T., Elsherbiny, D.A., Tadros, M.G., George, M.Y., 2025. Lycopene mitigates paclitaxel-induced cognitive impairment in mice; insights into Nrf2/HO-1, NF-κb/NLRP3, and GRP-78/ATF-6 axes. Progress in Neuro-Psychopharmacol. Biolog. Psychiatry 137, 111262.
Zhang, H., Zhao, Y., Cui, J.G., Li, X.N., Li, J.L., 2022. DEHP-induced mitophagy and mitochondrial damage in the heart are associated with dysregulated mitochondrial biogenesis. Food Chem. Toxicol. 161, 112818.
Zhang, K., Yang, J., Chen, L., He, J., Qu, D., Zhang, Z., Liu, Y., Li, X., Liu, J., Li, J., Xie, X., Wang, Q., 2023a. Gut microbiota participates in polystyrene microplastics-induced hepatic injuries by modulating the Gut-liver axis. ACS. Nano.
Zhang, Z., Song, W., Yan, R., 2023b. Gbp3 is associated with the progression of lupus nephritis by regulating cell proliferation, inflammation and pyroptosis. Autoimmunity 56, 2250095.
Zhao, B., Wu, J., Li, J., Bai, Y., Luo, Y., Ji, B., Xia, B., Liu, Z., Tan, X., Lv, J., Liu, X., 2020a. Lycopene alleviates DSS-induced colitis and behavioral disorders via mediating microbes-gut-brain axis balance. J Agr Food Chem 68, 3963–3975.
Zhao, T.X., Wei, Y.X., Wang, J.K., Han, L.D., Sun, M., Wu, Y.H., Shen, L.J., Long, C.L., Wu, S.D., Wei, G.H., 2020b. The gut-microbiota-testis axis mediated by the activation of the Nrf2 antioxidant pathway is related to prepuberal steroidogenesis disorders induced by di-(2-ethylhexyl) phthalate. Environ Sci Pollut R 27, 35261–35271.
Zhao, Y., Bao, R.K., Zhu, S.Y., Talukder, M., Cui, J.G., Zhang, H., Li, X.N., Li, J.L., 2021a. Lycopene prevents DEHP-induced hepatic oxidative stress damage by crosstalk between AHR-Nrf2 pathway. Environ. Pollut. 285, 117080.
Zhao, Y., Chang, Y., Ren, H., Lou, M., Jiang, F., Wang, J., Chen, M., Liu, S., Shi, Y., Zhu, H., Li, J., 2024. Phthalates induce neurotoxicity by disrupting the Mfn2-PERK axis-mediated endoplasmic reticulum–Mitochondria interaction. J. Agr. Food Chem. 72, 7411–7422.
Zhao, Y., Cui, J.G., Zhang, H., Li, X.N., Li, M.Z., Talukder, M., Li, J.L., 2021b. Role of mitochondria-endoplasmic reticulum coupling in lycopene preventing DEHP-induced hepatotoxicity. Food Funct. 12, 10741–10749.
Zhao, Y., Li, X.N., Zhang, H., Cui, J.G., Wang, J.X., Chen, M.S., Li, J.L., 2022. Phthalate-induced testosterone/androgen receptor pathway disorder on spermatogenesis and antagonism of lycopene. J. Hazard. Mater. 439, 129689.
Zhu, B., Gu, Z., Hu, H., Huang, J., Zeng, Z., Liang, H., Yuan, Z., Huang, S., Qiu, Y., Sun, X., Liu, Y., 2025. Altered gut microbiota contributes to acute-Respiratory-distress-syndrome-related depression through microglial neuroinflammation. Research. 8, 636.